Supporting Information

Functionalized DNA-Origami-Protein Nanopores Generate Large Transmembrane Channels with Programmable Size-Selectivity

Qi Shen[‡,a,b,c], Qiancheng Xiong[‡,a,b], Kaifeng Zhou[c], Qingzhou Feng[a,b], Longfei Liu[a,b], Taoran Tian [a], Chunxiang Wu[c], Yong Xiong[c], Thomas J. Melia[a], C. Patrick Lusk[a], and Chenxiang Lin[*,a,b,d]

[a] Department of Cell Biology, Yale School of Medicine, 333 Cedar Street, New Haven, Connecticut 06520, United States

[b] Nanobiology Institute, Yale University, 850 West Campus Drive, West Haven, Connecticut 06516, United States

[c] Department of Molecular Biophysics and Biochemistry, Yale University, 266 Whitney Avenue, New Haven, Connecticut 06511, United States

[d] Department of Biomedical Engineering, Yale University, 17 Hillhouse Ave, New Haven, Connecticut 06511, United States

* Email: chenxiang.lin@yale.edu

[‡] These authors contributed equally.

Contents

MATERIALS AND METHODS

DNA-origami design, assembly, and modification.
The DNA-origami ring was designed in caDNAno[1] (**Figure S2**). Unmodified staple strands were purchased from Integrated DNA Technologies, Inc. (IDTDNA) in 96-well plates, with concentrations normalized to 100 μM. Staple strands with Cy3 fluorescence modifications were purchased in dry powder form with HPLC purification from IDTDNA. The p8064 scaffold strand, an M13mp18-based single-stranded DNA, was prepared as previously described.[2]

The DNA ring (**Figure 1** and **S2**) was assembled from the p8064 scaffold strand (50 nM), a pool of staple strands (200 nM each) in a 1× TE buffer (5 mM Tris•HCl, 1 mM EDTA, pH 8.0) containing 16 mM $MgCl_2$, using a 36-hour annealing program (80−65 °C, -1 °C/5 min; 64−24 °C, -1 °C/50 min; 15 °C hold).

The folded structures were purified by rate-zonal centrifugation.[3] Typically, 500 μl of the assembled product was combined with 1× TE buffer containing 40% glycerol and 10 mM $MgCl_2$ to reach a final glycerol concentration of 10%, loaded on top of a 15−45% (v/v) quasi-linear glycerol gradient in a polycarbonate centrifuge tube (13×51 mm, Beckman Coulter Inc.), and spun at 50 krpm on a Beckman SW-55-Ti rotor for 60 min at 4 °C. The tube contents were fractionated from top to bottom (200 μL per fraction). Generally, 5 μL of each fraction was loaded onto a 1.5% agarose gel containing 0.5 μg/mL ethidium bromide (EtBr) and run in 0.5 × TBE (45 mM Tris-Base, 45 mM boric acid, and 1 mM EDTA), 10 mM $MgCl_2$ for 2 hours at 5 V/cm. After image analysis on a Typhoon FLA 9500 imager (Cytiva), the fractions containing well-formed monomeric DNA origami were combined and concentrated using Amicon Ultra-0.5 mL Centrifugal Filters with 30-kD NMWL (Millipore Sigma). Origami concentrations were determined using a NanoDrop 2000 (Thermo Fisher Scientific). The concentrated monomers were stored in 1× TE buffer, 10 mM $MgCl_2$ at -20 °C.

To label the DNA ring with PLY and Cy3, 2880 nM of anti-handle-conjugated PLY (see the subsection "Preparation of DNA-conjugated PLY and Nsp1" for details) and 240 nM of Cy3-modified anti-handles (see **Table S2** for sequence) were mixed with 20 nM of purified DNA-origami ring module in 1× TE buffer containing 10 mM $MgCl_2$ at 37 °C for 2 hours. To remove excess free DNA-conjugated PLY and Cy3-modified oligonucleotides from PLY-DNA ring constructs, we combined the product with 1× TE buffer containing 40% glycerol and 10 mM $MgCl_2$ to reach a final glycerol concentration of 10%. This mixture was then loaded on top of a 15−45% (v/v) quasi-linear glycerol gradient in a polycarbonate centrifuge tube (5×41 mm, Beckman Coulter Inc.), and spun at 48 krpm on a Beckman SW-55-Ti rotor for 60 min at 4 °C. The tube contents were fractionated from top to bottom (50 μL per fraction). Typically, 5 μL of each fraction was then loaded onto a 1.5% agarose gel containing 0.5 μg/mL EtBr and run in 0.5 × TBE, 10 mM $MgCl_2$ for 2 hours at 5 V/cm. After image analysis on a Typhoon FLA 9500 imager, the fractions containing purified PLY-DNA rings were combined and stored in LoBind protein tubes (Eppendorf) at -80 °C. To prepare Nsp1-modified PLY-DNA rings, we mixed anti-handle-conjugated Nsp1 and the purified PLY-DNA origami at a molar ratio of anti-handle-Nsp1:PLY-DNA = 54:1 and incubated them at room temperature for 2 hrs.

Protein expression and purification
The PLY gene[4] (see **Table S1** for protein sequence) from *Streptococcus pneumoniae* was cloned as 6× His-tagged PLY constructs into a pET-28a-derived vector (Novagen) and expressed in BL21-Gold (DE3). Cells were grown in LB medium at 37 °C in a shaking incubator until they reached an OD600 of 1.0. Protein

expression was then induced with 1 mM IPTG for 4 hrs at 37 °C before collection by centrifugation. Cell pellets were stored at -80°C until use. Then, they were resuspended in lysis buffer (1x PBS, 0.5 mM TCEP, 0.1 mM PMSF, 1x Roche cOmplete protease inhibitors), and lysed in a cell disruptor (EmulsiFlex-C3, Avestin). Whole-cell lysates were spun at 35 krpm for 45 min in a Type 45 Ti rotor (Beckman Coulter), and the supernatant was decanted. The lysate was applied to a 0.45 µm filter and subsequently to a 5 mL HisTrap column (Cytiva) on an ÄKTA system (Cytiva) at a flow rate of 1 mL/min. The column was washed with Buffer A (1× PBS, 0.5 mM TCEP, 25 mM imidazole) and eluted on a gradient of elution buffer (1× PBS, 0.5 mM TCEP, 500 mM imidazole). Purified PLY concentration was determined by Nanodrop (Thermo Fisher Scientific). Eluate was spiked with 10% glycerol, flash-frozen in liquid nitrogen, and stored at -80°C until use.

The gene encoding Nsp1 FG-domains (amino acids 2-603) from *Saccharomyces cerevisiae* were cloned as a 10×His-MBP-sumo-TEV-nucleoporins-SNAP construct[5] (see **Table S1** for protein sequence) in a pET28a vector (Novagen) and expressed in *Escherichia coli* strain BL21-Gold (DE3). Cells were grown in LB medium at 37°C, shaking, until OD ~0.8, and protein expression was induced with 1 mM IPTG for 5 hr at 25°C before collection by centrifugation. Cell pellets were frozen at -80 °C until use. Nsp1 was purified using a HisTrap column as reported previously.[5]

Preparation of DNA-conjugated PLY and Nsp1

Maleimide-DNA preparation

5'-labeled amino-DNA oligonucleotides (see **Table S2** for sequence) were purchased from IDTDNA, resuspended in Milli-Q ultrapure water, and buffer exchanged into 10 mM HEPES, pH 7.4 using a Micro Bio-spin 6 column (Bio-Rad) to remove free amines. Sulfo-SMCC (Pierce and G-Biosciences) was resuspended in de-ionized H_2O at 50 °C. sulfo-SMCC (2 mM) was reacted with amino-DNA (200 µM) for 3 hr at 37 °C in 100 mM HEPES, pH 7.4, and purified by ethanol precipitation. Dried maleimide-DNA pellets were stored at -20°C until use.

Benzylguanine (BG)-DNA preparation

5'-labeled amino-DNA oligonucleotides (see **Table S2** for sequence) were purchased from IDTDNA, were resuspended in Milli-Q ultrapure water at 2 mM concentration. BG-GLA-NHS (New England Biolabs) was dissolved in DMSO at 20 mM. Amino-DNA (2 mM) and BG-GLA-NHS (20 mM) were mixed in a 1:3 volume ratio in a 67 mM HEPES, pH 8.5 buffer, and incubated at room temperature for 1 hr. BG-DNA was then purified from excess BG-GLA-NHS by ethanol precipitation. Dried BG-DNA pellets were stored at -20 °C until use.

Protein-DNA conjugation

To conjugate DNA anti-handle to PLY, maleimide-DNA pellets were resuspended in 10 mM HEPES, pH 7.4, and mixed with affinity purified PLY in 1× PBS buffer at a final concentration of 20 µM maleimide-DNA and 10 µM PLY (2:1). This reaction mixture was incubated at 37 °C for 3 hr.

To conjugate DNA anti-handle to Nsp1, BG-DNA pellets were resuspended in Milli-Q ultrapure water and mixed with purified Nsp1 in 1× PBS buffer at a final concentration of 20 µM BG-DNA and 10 µM Nsp1 (2:1). This reaction mixture was incubated at 25 °C for 2 hr.

For both types of reactions, excess DNA was removed from the DNA-conjugated proteins by size exclusion chromatography (SEC) using a Superdex 200 10/300 column (GE Healthcare) in 1× PBS buffer (**Figure S1**). Conjugation efficiency was verified by SDS-PAGE. Precast gels (4–12% NuPAGE, Thermo Fisher Scientific) were run in MES-SDS or MOPS-SDS buffer at 20V/cm for 35 min at room temperature and stained using Coomassie Brilliant Blue G-250 (Thermo Fisher Scientific).

Hemolysis assay

PLY's hemolytic activity was tested by lysing sheep red blood cells (SRBC).[6] Purified PLY and PLY-DNA ring were serially diluted in hemolysis buffer (1× PBS pH 7.0, 10 mM $MgCl_2$, 0.01% (v/v) BSA) in final volumes of 100 µl and incubated for 30 min at 37°C with 100 µl of an SRBC (Innovative Research) suspension (10^8/ml). This mixture was spun at 5,000 × g for 10 min at 25 °C. The absorbance of supernatant at 405 nm was used to monitor hemoglobin release. The amount of toxin required to lyse 50% of erythrocytes (EC_{50}) was determined using the OD_{405} of SRBC supernatant treated by 1% Triton-X100 as a reference for 100% lysis. Three independent measurements were performed for each sample.

SDS-agarose gel electrophoresis

Samples were loaded in an SDS-agarose gel (1.5% agarose in 0.5× TBE, 10 mM $MgCl_2$, and 0.05% SDS). Electrophoresis was carried out at 5.8 V/cm for 120 min in 0.5× TBE buffer containing 10 mM $MgCl_2$ and 0.05% SDS. For EtBr staining, the gel was soaked in de-ionized H_2O, shaken for 1 hr to remove SDS, and then submerged in an EtBr solution (Sigma-Aldrich, 20,000× dilution in H_2O to 0.5 µg/mL) for 1 hr. Gels were destained for 1 hour in de-ionized H_2O before imaging. Gels were imaged on a Typhoon FLA 9500 scanner for the EtBr fluorescence.

Preparation of large unilamellar vesicles (LUVs)

LUVs composed of 70% 1,2-dioleoyl-sn-glycero-3-phosphocholine (DOPC) and 30% ovine cholesterol (Avanti Polar Lipids, Inc.) were produced by lipid-film rehydration and extrusion. Briefly, appropriate amounts of lipids in chloroform were mixed in glass tubes and dried in nitrogen gas for 30 min and under vacuum overnight. The lipid film was then suspended in 500 µL of hydration buffer (50 mM Tris•HCl, 150 mM NaCl, 15 mM $MgCl_2$, pH 7.0) by agitation to achieve a final lipid concentration of 1 mg/mL. The suspended lipids were frozen-thawed in plastic centrifuge tubes for eight cycles, each consisting of 15-s flash-freezing in liquid nitrogen and 2-min water-bathing at 37 °C. Final homogenization was achieved through 40 forward-and-back extrusion pumps using a LiposoFast system (Avestin, Inc.) with first a 200-nm Whatman Nuclepore track-etched membrane followed by a 100-nm membrane (Cytiva). The final LUVs were stored at 4 °C for no more than 2 weeks before usage. LUVs used for Cryo-EM were always freshly prepared.

Preparation of giant unilamellar vesicles (GUVs)

GUVs composed of 69.2% DOPC, 30% ovine cholesterol and 0.8% 1,2-dioleoyl-sn-glycero-3-phosphoethanolamine-N-(Cyanine 5) (Cy5-PE) (Avanti Polar Lipids, Inc.) were produced by electroformation[7] using a Vesicle Prep Pro (Nanion Technologies). Briefly, to form thin lipid films, 1 mg/mL lipid solution in chloroform was spotted within an 18 mm O-ring chamber on the conducting face of an indium-tin-oxide-coated glass slide on a 45 °C heat plate. The lipids were then covered with foil and placed in a vacuum chamber for at least 1 hour. Subsequently, the O-ring chamber was filled with about 275 µL of sucrose solution containing 0.03% w/v sodium azide at an osmolarity of 362 mOsm (measured via a Thomas Scientific Micro-Osmette osmometer), which is 20 mOsm lower than the hydration buffer (382 mOsm), to prevent vesicle bursting. The filled chamber was shielded from light with aluminum foil, and the Vesicle Prep Pro machine then ran a base protocol (37 °C, 8 Hz, 1.1 V, 45 min Rise, 60 min Main, 45 min Fall). The resulting GUVs were released from glass with gentle tapping and carefully extracted using a cut 1000 µL micropipette tip and stored in LoBind tubes (Eppendorf) at 4 °C.

Transmission electron microscopy (TEM)

For negative-stain TEM, a drop of the sample (5 µL) was deposited on a glow-discharged formvar/carbon-coated copper grid (Electron Microscopy Sciences), incubated for 1 min, and blotted away. The grid was first rinsed twice with 5 µL 1× TE buffer containing 10 mM $MgCl_2$, then stained briefly for 5 s with 5 µL 2% (w/v) uranyl formate, before blotting away and stained a second time for 1 min. Images were acquired

on a JEOL JEM-1400Plus microscope (acceleration voltage: 80 kV) with a bottom-mount 4k×3k CCD camera (Advanced Microscopy Technologies). Diameters of PLY-DNA pores were determined using ImageJ (version 1.52b)[8].

Cryogenic electron microscopy (Cryo-EM)

A drop (3 µl) of sample was adsorbed on glow-discharged holey carbon grids (Quantifoil MicroTools). Grids were then blotted and plunge-frozen in liquid ethane using FEI Vitrobot operating at 100% humidity, 22 °C temperature, and 5 seconds blot time. Imaging was performed on a Glacios microscope (Thermo Fisher Scientific) equipped with a Gatan K3 Summit direct detector in super-resolution mode, operated at 200 kV. The images were collected at magnifications of 22,000× and 36,000×, using a defocus range of −2 to −3 µm. Automated data collection was performed using SerialEM 3.873. Diameters of PLY-DNA pores were determined in ImageJ (version 1.52b).

Confocal fluorescence microscopy

A 10 µL drop of 2 mg/mL bovine serum albumin (BSA) was placed on an uncoated glass-bottom dish (MatTek Corporation) for 20 min and washed with hydration buffer 8 times. Hydration buffer was spotted along the dish walls to mitigate evaporation. For transferring GUVs, 20 µL micropipette tips were cut transversely to increase tip entry diameter and reduce shear stress on GUVs.

For a typical permeability assay, at the time t = 0 min, a 10 µL drop from a freshly mixed 15 µL liquid (containing 1.5 µL of GUVs in sucrose, 1.5 µL of 10 µM FITC-dextran (Sigma-Aldrich), 3 µL of 5 nM Cy3-labeled PLY-DNA rings or 20 nM Cy3-labeled DNA-origami control, and 9 µL of hydration buffer) was dispensed on the BSA-coated region of the glass-bottom dish. The GUVs were imaged under a Leica TCS SP8 confocal microscope using an HC PL APO CS2 63× OIL objective lens. All experiments were conducted at room temperature.

To induce photobleaching for fluorescence recovery after photobleaching (FRAP) analysis, we set a white-light laser to scan over the region of interest with 484 nm, 492 nm, and 500 nm at 100/100 of 70% laser power for 8.67 s. Recovery after photobleaching was measured by collecting frames as fast as possible for the first 20 frames (one about every 433 ms) and then every 15 s. Fluorescence intensities for the region of interest and surrounding background were extracted using the Leica Application Suite X (version 3.7.5.24914) and then fitted using MATLAB (version R2022a, 9.12.0.1884302, 64-bit) after background subtraction and normalization (**Figure S10**).

The FITC-dextran (Millipore Sigma) used in this study are 20 kDa (FITC/glucose (mol/mol) = 0.003-0.020), 40 kDa (FITC/glucose (mol/mol) = 0.003-0.020), 70 kDa (FITC/glucose (mol/mol) = 0.004), and 150 kDa (FITC/glucose (mol/mol) = 0.004).

SUPPLEMENTAL FIGURES

Figure S1. Purification and verification of PLY-anti-handle conjugates. **(A)** An SEC profile of DNA anti-handles conjugated with PLY monomers. **(B)** The highlighted fractions from (**A**) were analyzed by SDS-PAGE to determine conjugation efficiency and the fractions (f2–f4) were combined for subsequent experiments.

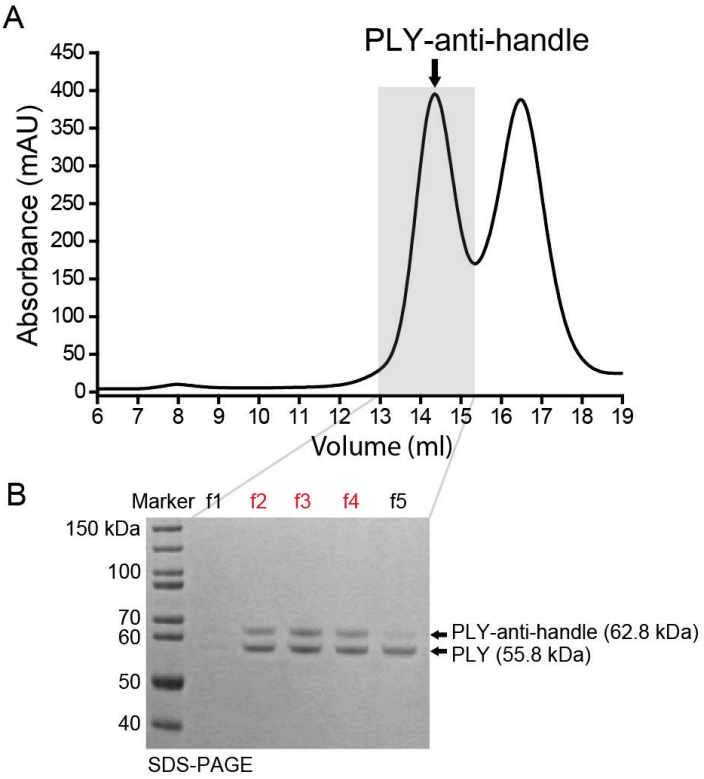

Figure S2. Design of the DNA-origami ring. Cross-section view of the DNA ring (top) and the caDNAno strand diagram (bottom). Red (48 bottom handles for DNA-conjugated PLY hybridization), grey (36 inner handles for hybridization of DNA-conjugated Nsp1), blue (8 outer handles for hybridization of Cy3-labeled DNA), green (p8064 DNA scaffold). Handle sequences can be found in **Table S2**.

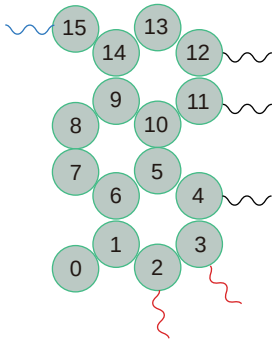

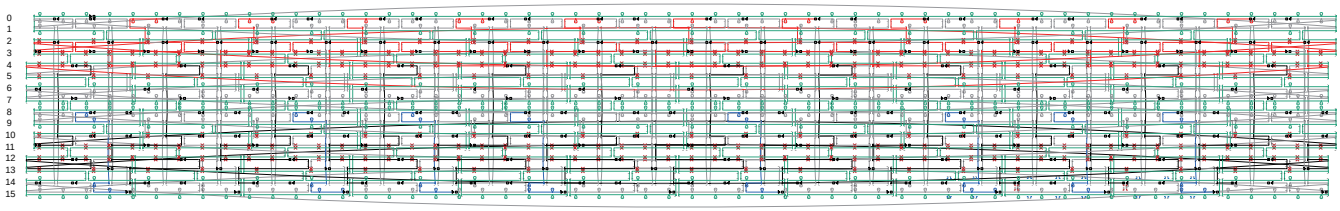

Figure S3. **(A)** Agarose gel electrophoresis of the DNA ring after rate-zonal purification. Fractions in red contain well-folded DNA structures selected for use in subsequent experiments. U: unpurified sample. M: 1 kb DNA ladder. **(B)** Agarose gel electrophoresis of PLY and Cy3 modified DNA rings after rate-zonal purification. The fraction in red was selected for use in subsequent experiments. U: unpurified sample. M: 1 kb DNA ladder. **(C)** Agarose gel electrophoresis confirming the incorporation of DNA-conjugated PLY to origami rings.

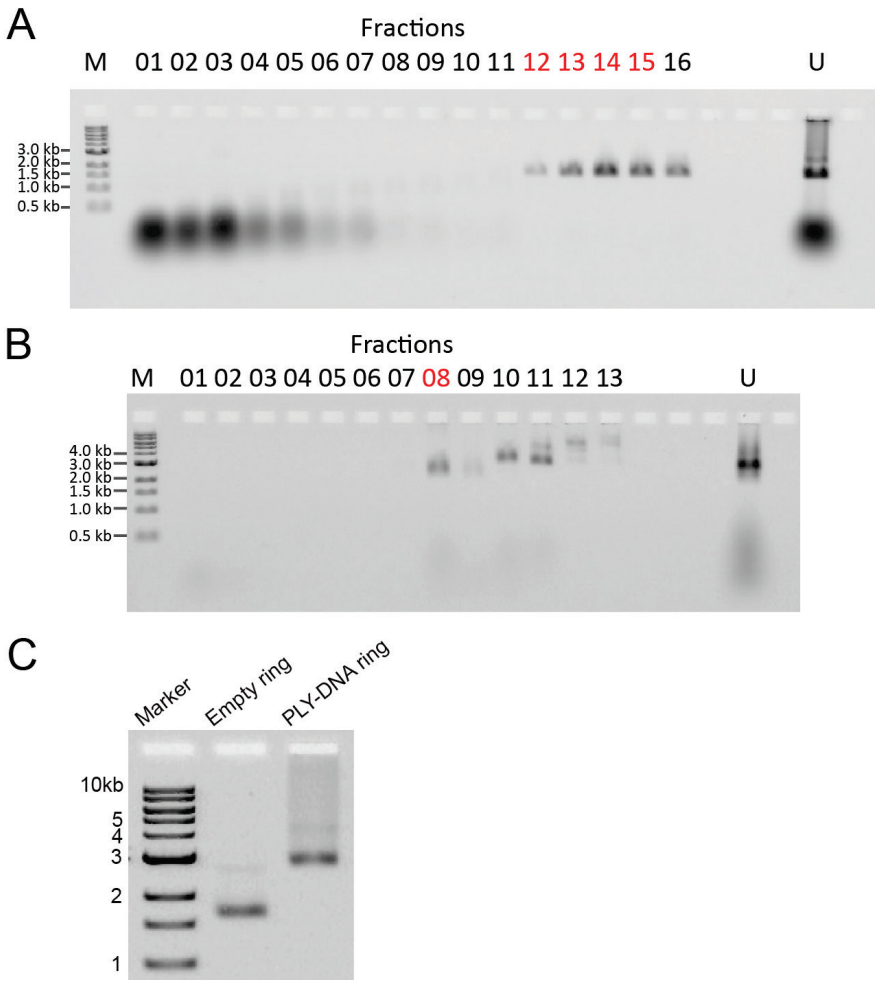

Figure S4. A negative-stain electron micrograph showing rate-zonal purified PLY-DNA rings.

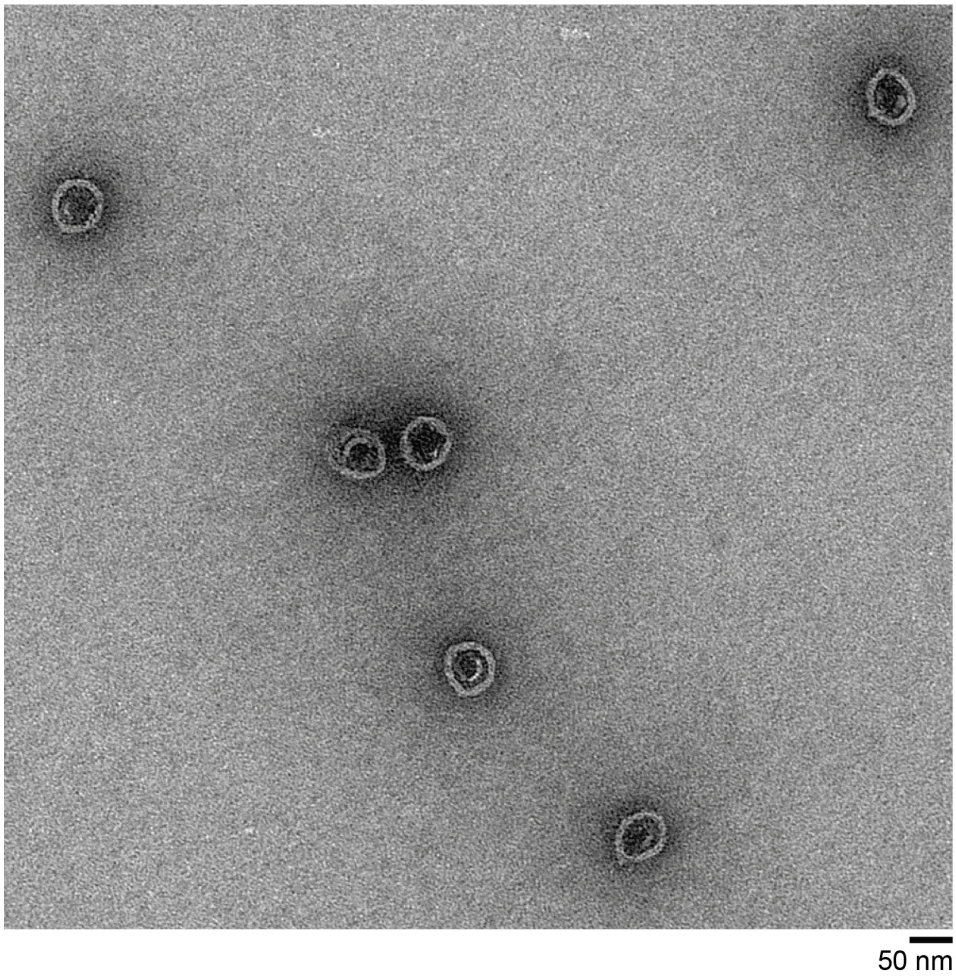

Figure S5. Representative electron micrographs of DNA-corralled or free PLY pores on the membrane. Representative negative-stain TEM (**A**) and cryo-EM (**B**) micrographs used for measuring the PLY-DNA pore inner diameter. In ImageJ, we first used the "Oval" selection tool (dashed circle in yellow) to measure the inner area of the PLY-DNA pores on LUV membranes, and then calculated their diameters as $2\sqrt{Area/\pi}$. (**C**) Representative negative-stain TEM micrographs used for measuring the inner diameters of PLY-only pores.

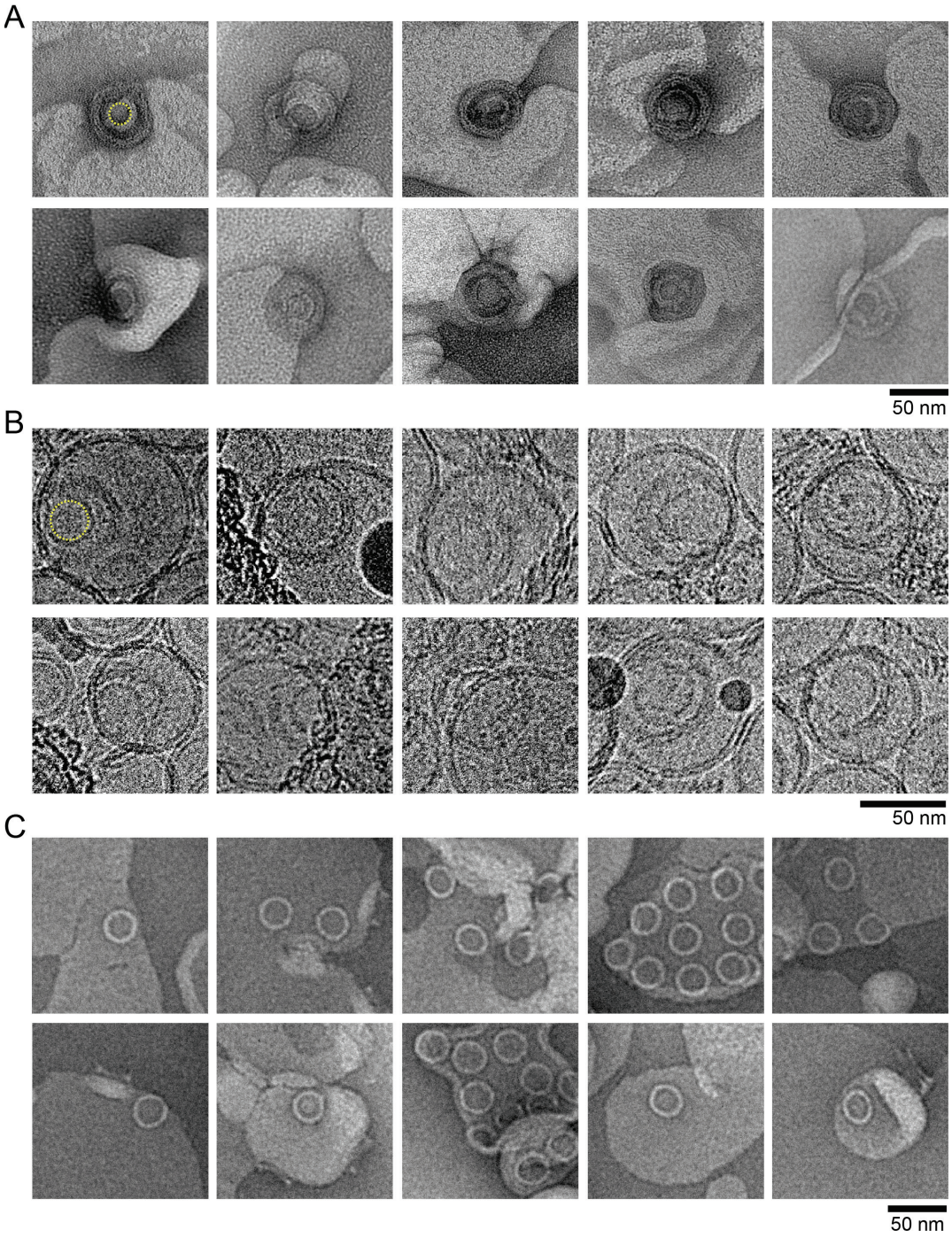

Figure S6. A gallery of cryo-EM micrographs showing LUV-bound PLY-DNA rings.

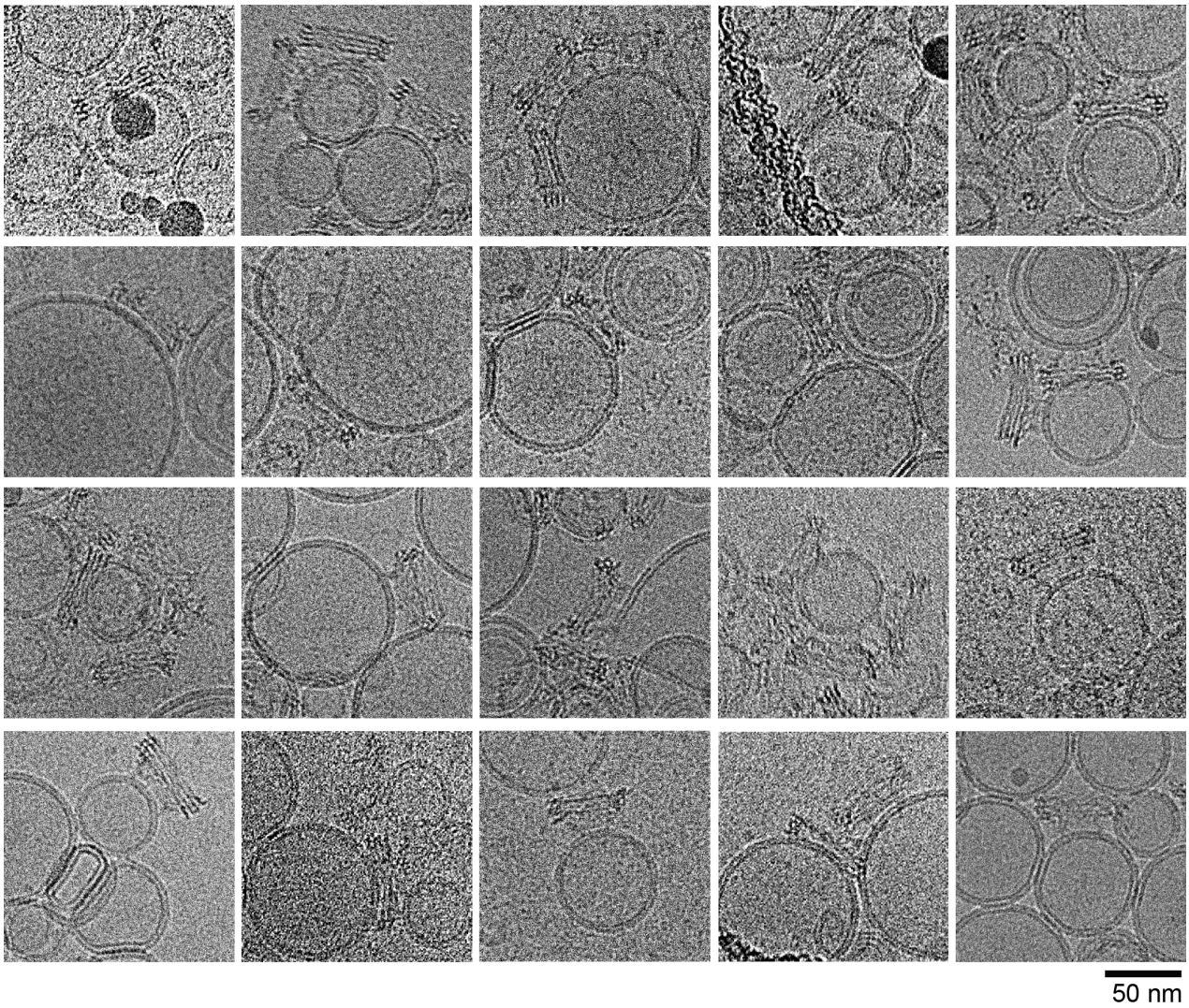

Figure S7. Estimating the surface coverage of GUVs by PLY-DNA rings by their Cy3 labels. The average Cy3 intensity outside the GUV was first measured (n=16) using a control sample of GUVs mixed with Cy3-labeled rings without PLY. Subsequently, in the Cy3 channel image of a GUV with Cy3-labeled PLY-DNA rings attached (acquired under the same conditions as the control), the GUV interior was selected in ImageJ and cleared. The PLY-labeled and PLY-free DNA rings have the same number of Cy3-modification sites (8 each).

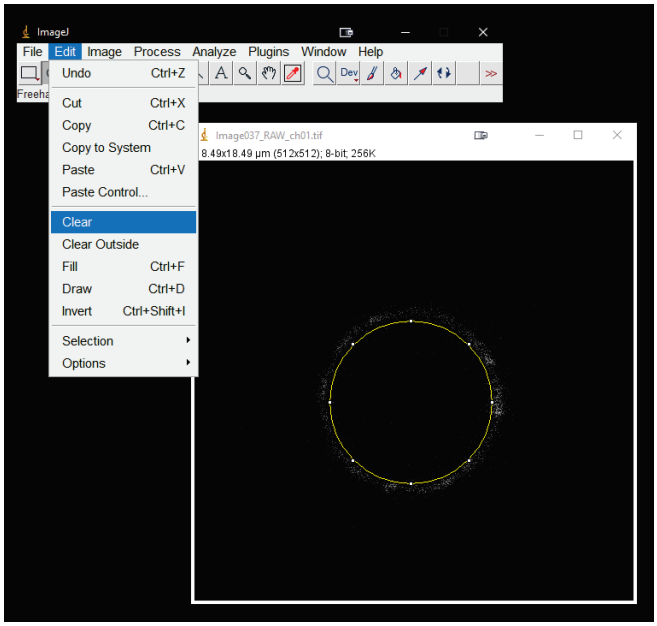

The GUV was then selected, and its mean Cy3 intensity and area were measured. Surface coverage density was then calculated using the average background intensity, the known concentration of Cy3-labeled DNA ring control in the background (6 nM) and the outer diameter of the DNA ring (62 nm). The details are as follows.

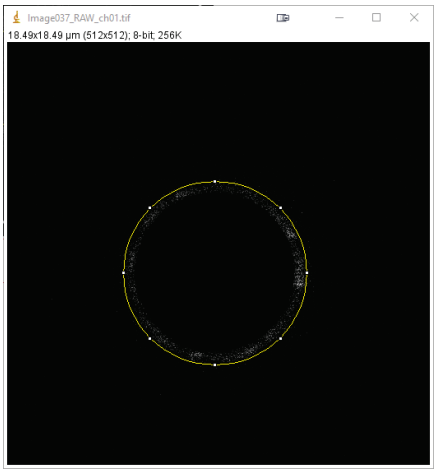

The total fluorescence intensity of PLY-DNA ring captured in the image ($total_{GUV}$) can be described as

$$total_{GUV} = k \times density \times L \times \Delta z$$

where k is a constant relating the number of DNA origami with their fluorescence intensity, *density* is the number of DNA origami per unit of area, L is the length of the GUV's equator, Δz is the measured optical section thickness.

Similarly, the total fluorescence intensity of PLY-free DNA ring in the background ($total_{background}$) can be described as

$$total_{background} = k \times c \times S \times \Delta z$$

where c is the concentration of Cy3-labeled, PLY-free DNA ring in solution (i.e., 6 nM), S is the area of the selected background region.

Thus, the surface coverage density (μm^{-2}) can be calculated by

$$density = \frac{total_{GUV}}{total_{background}} \times \frac{c \times S}{L}$$

where c = 6 nM and all other parameters were measured using ImageJ.

The surface coverage (%) can be calculated by

$$surface\ coverage = density \times Area_{\ DNA\ ring} \times 100\%$$

$$Area_{\ DNA\ ring} = \pi \times (0.5 \times D)^2$$

where D is the outer diameter of DNA origami (62 nm).

Figure S8. Purification and validation of the four FITC-dextran species used in this study. **(A)** SEC profiles of unpurified FITC-dextran of various sizes. The highlighted fractions were collected for use in the permeability and FRAP assays. **(B)** Purified dextrans validated by a second run through SEC.

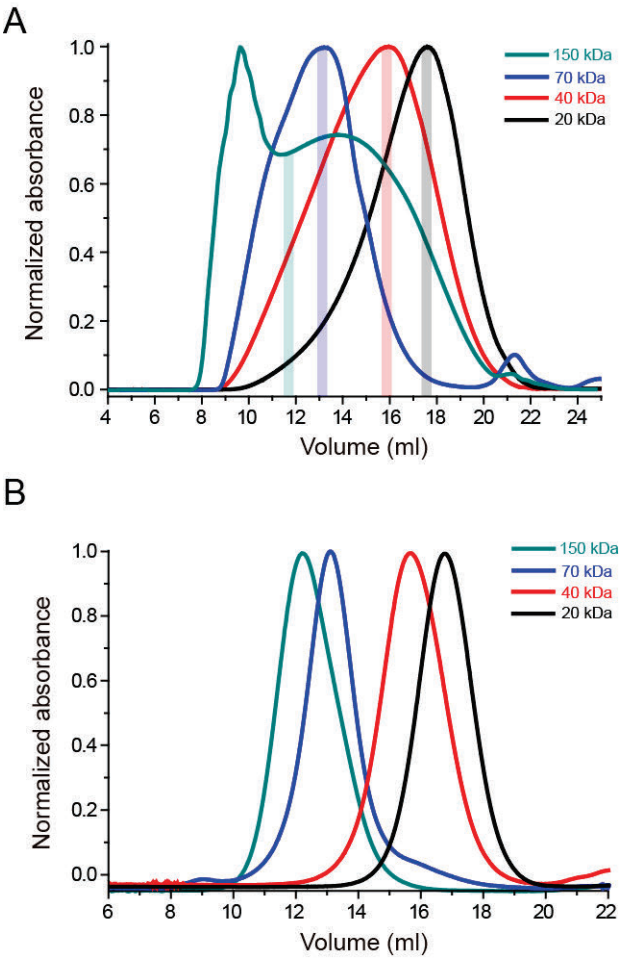

Figure S9. Representative GUVs (red, Cy5-PE) imaged under confocal microscopy after the addition of dextrans (green) of various molecular weights and PLY-DNA rings (cyan) in the surrounding buffer. Scale bar: 5 μm.

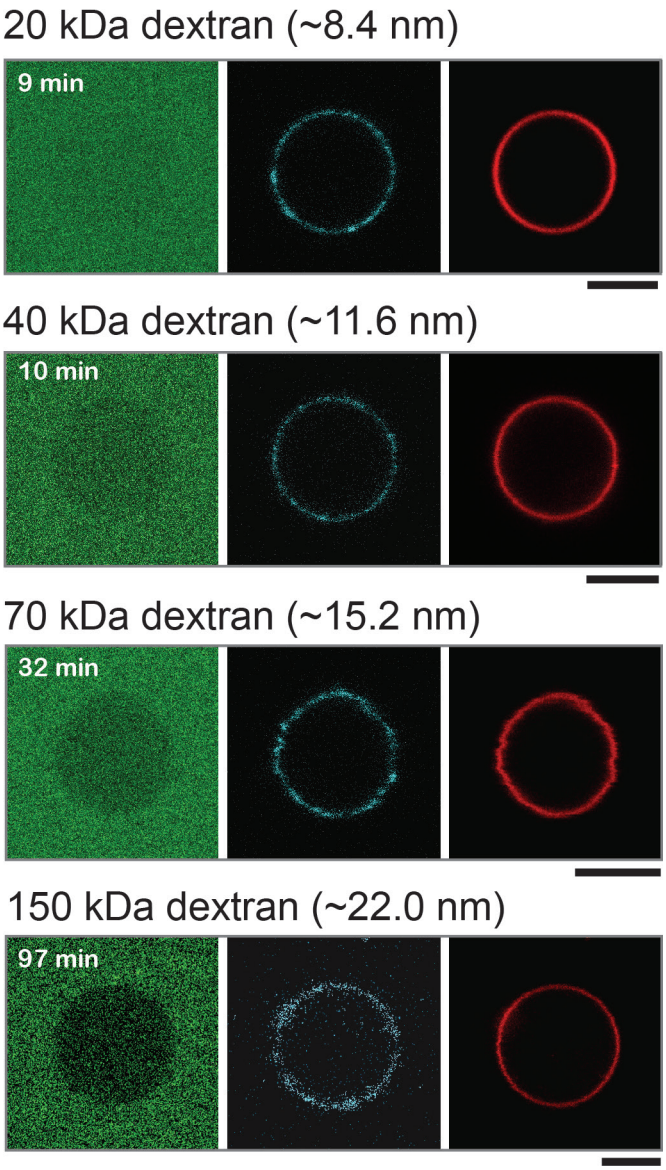

Figure S10. Image analysis of the FRAP assay. Post-photobleaching, FITC-dextran (green) intensities of the GUV interior (ROI 01 in red; mean intensity = $\boldsymbol{I_{in}}$) and surrounding areas (ROI 02, 03, 04, 05, all in purple, mean intensity = $\boldsymbol{I_{out}}$) were measured. The time-lapsed intensity differences $\boldsymbol{1 - (I_{out} - I_{in}) / I_{out}}$ was then normalized to a range of [0,1]. The initial rate of macromolecule influx was represented by the slope (***K***) of the initial best-fit linear line from at least 20 data points. As the apparent rate of initial recovery (i.e., ***K***) is proportional to the surface area of GUV (a larger surface area contains more pores) and inversely proportional to the volume of GUV, the ***K*** value from each FRAP dataset was normalized by multiplying ***r***, the radius of the GUV tested.

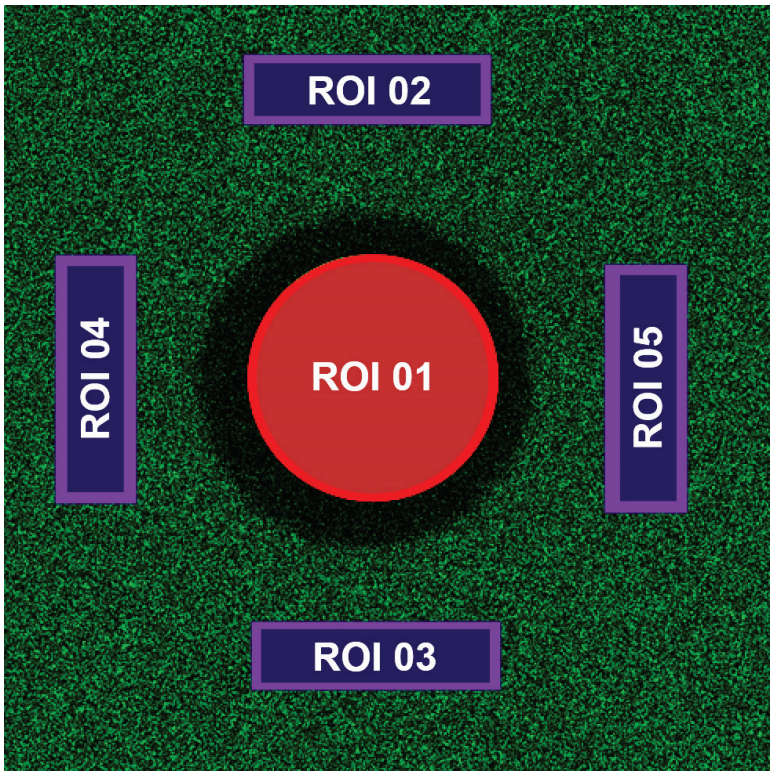

Figure S11. Representative GUVs (red, Cy5-PE) mixed with ungated or Nsp1-modified PLY-DNA rings (cyan) imaged under confocal microscopy after the addition of 70 kDa dextrans (green). Scale bar: 5 μm.

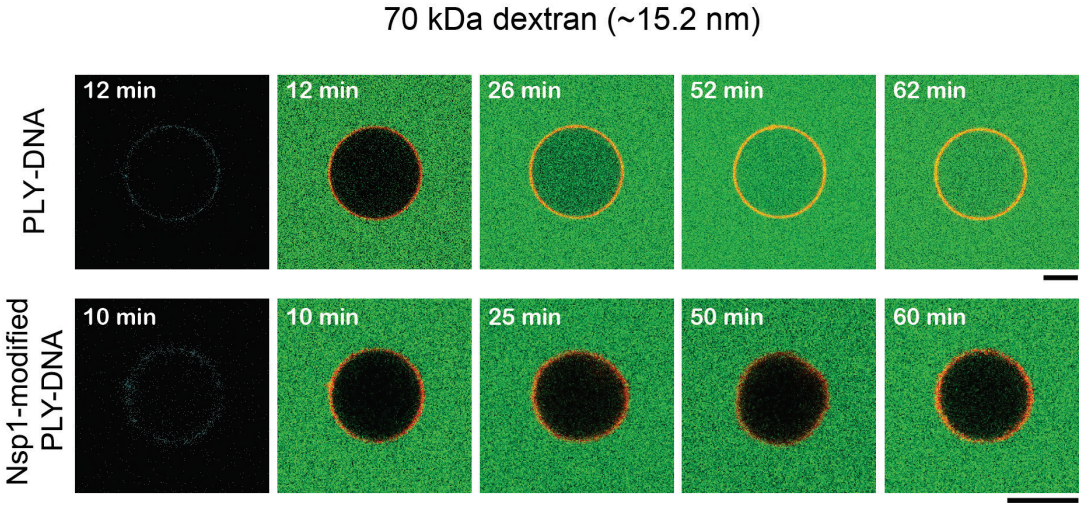

SUPPLEMENTAL TABLES

Table S1. PLY and Nsp1 sequences. The DNA conjugation site is highlighted in red.

PLY sequence (His-TEV-Cys-PLY$_{C428A}$)
MGSSHHHHHHSSGENLYFQGHMASCSHMANKAVNDFILAMNYDKKKLLTHQGESIENRFIKEGNQLPD EFVVIERKKRSLSTNTSDISVTATNDSRLYPGALLVVDETLLENNPTLLAVDRAPMTYSIDLPGLASSDSF LQVEDPSNSSVRGAVNDLLAKWHQDYGQVNNVPARMQYEKITAHSMEQLKVKFGSDFEKTGNSLDID FNSVHSGEKQIQIVNFKQIYYTVSVDAVKNPGDVFQDTVTVEDLKQRGISAERPLVYISSVAYGRQVYLK LETTSKSDEVEAAFEALIKGVKVAPQTEWKQILDNTEVKAVILGGDPSSGARVVTGKVDMVEDLIQEGS RFTADHPGLPISYTTSFLRDNVVATFQNSTDYVETKVTAYRNGDLLLDHSGAYVAQYYITWDELSYDHQ GKEVLTPKAWDRNGQDLTAHFTTSIPLKGNVRNLSVKIREATGLAWEWWRTVYEKTDLPLVRKRTISI WGTTLYPQVEDKVEND
Nsp1 sequence (His-MBP-sumo-TEV-Nsp1-SNAP)
MGHHHHHHHHHHKIEEGKLVIWINGDKGYNGLAEVGKKFEKDTGIKVTVEHPDKLEEKFPQVAATGD GPDIIFWAHDRFGGYAQSGLLAEITPDKAFQDKLYPFTWDAVRYNGKLIAYPIAVEALSLIYNKDLLPNP PKTWEEIPALDKELKAKGKSALMFNLQEPYFTWPLIAADGGYAFKYENGKYDIKDVGVDNAGAKAGLT FLVDLIKNKHMNADTDYSIAEAAFNKGETAMTINGPWAWSNIDTSKVNYGVTVLPTFKGQPSKPFVGV LSAGINAASPNKELAKEFLENYLLTDEGLEAVNKDKPLGAVALKSYEEELAKDPRIAATMENAQKGEIM PNIPQMSAFWYAVRTAVINAASGRQTVDEALKDAQTASMSDSEVNQEAKPEVKPEVKPETHINLKVSD GSSEIFFKIKKTTPLRRLMEAFAKRQGKEMDSLRFLYDGIRIQADQTPEDLDMEDNDIIEAHREQIGGHME NLYFQGNFNTPQQNKTPFSFGTANNNSNTTNQNSSTGAGAFGTGQSTFGFNNSAPNNTNNANSSITPAFG SNNTGNTAFGNSNPTSNVFGSNNSTTNTFGSNSAGTSLFGSSSAQQTKSNGTAGGNTFGSSSLFNNSTNS NTTKPAFGGLNFGGGNNTTPSSTGNANTSNNLFGATANANKPAFSFGATTNDDKKTEPDKPAFSFNSSV GNKTDAQAPTTGFSFGSQLGGNKTVNEAAKPSLSFGSGSAGANPAGASQPEPTTNEPAKPALSFGTATS DNKTTNTTPSFSFGAKSDENKAGATSKPAFSFGAKPEEKKDDNSSKPAFSFGAKSNEDKQDGTAKPAFSF GAKPAEKNNNETSKPAFSFGAKSDEKKDGDASKPAFSFGAKPDENKASATSKPAFSFGAKPEEKKDDNS SKPAFSFGAKSNEDKQDGTAKPAFSFGAKPAEKNNNETSKPAFSFGAKSDEKKDGDASKPAFSFGAKSD EKKDSDSSKPAFSFGTKSNEKKDSGSSKPAFSFGAKPDEKKNDEVSKPAFSFGAKANEKKESDESKSAFS FGSKPTGKEEGDGAKAAISFGAKPEEQKSSDTSKPAFTFGAQKDNEKKTEESKLMDKDCEMKRTTLDSP LGKLELSGCEQGLHEIKLLGKGTSAADAVEVPAPAAVLGGPEPLMQATAWLNAYFHQPEAIEEFPVPAL HHPVFQQESFTRQVLWKLLKVVKFGEVISYQQLAALAGNPAATAAVKTALSGNPVPILIPCHRVVSSSG AVGGYEGGLAVKEWLLAHEGHRLGKPGLG

Table S2. Handle and anti-handle sequences.

Outer “handles” for Cy3 modification	5'-CTTCACACCACACTCCATCTA-3'
Cy3-labeled “anti-handles”	5'-/Cy3/TAGATGGAGTGTGGTGTGAAG-3'
Bottom “handles” for DNA-conjugated PLY hybridization	5'- CTGATGATATTGATTGAAATG-3'
5’-amino-labeled “anti-handles” for PLY conjugation	5'-/AmMC6 /CATTTCAATCAATATCATCAG-3'
Inner “handles” for DNA-conjugated Nsp1 hybridization	5'-AAATTATCTACCACAACTCAC-3'
5’-amino-labeled “anti-handles” for Nsp1 conjugation	5'-/5AmMC6 /GTGAGTTGTGGTAGATAATTT-3'

STATISTICAL TESTS

Figure 3C. Comparisons of dextrans through PLY-DNA pores.

Left ****: $P < 0.0001$, a Mann–Whitney test ($U = 17$, two-tailed) comparing 20 kDa dextran (median = 7.31 $nm \cdot min^{-1}$, $n = 19$) and 40 kDa dextran (median = 1.22 $nm \cdot min^{-1}$, $n = 20$).

Right ****: $P < 0.0001$, a Mann–Whitney test ($U = 9$, two-tailed) comparing 40 kDa dextran (median = 1.22 $nm \cdot min^{-1}$, $n = 20$) and 70 kDa dextran (median = 0.50 $nm \cdot min^{-1}$, $n = 17$).

Figure 4F. Comparisons of dextrans through PLY-DNA and Nsp1-modified PLY-DNA pores.

Left ****: $P < 0.0001$, a Mann–Whitney test ($U = 17$, two-tailed) comparing 20 kDa dextran through PLY-DNA pores (median = 7.31 $nm \cdot min^{-1}$, $n = 19$, same dataset as in Figure 3C) and through Nsp1-modified PLY-DNA pores (median = 1.64 $nm \cdot min^{-1}$, $n = 16$).

Right ****: $P < 0.0001$, a Mann–Whitney test ($U = 34$, two-tailed) comparing 40 kDa dextran through PLY-DNA pores (median = 1.22 $nm \cdot min^{-1}$, $n = 20$, same dataset as in Figure 3C) and through Nsp1-modified PLY-DNA pores (median = 0.50 $nm \cdot min^{-1}$, $n = 16$).

Top ****: $P < 0.0001$, a Mann–Whitney test ($U = 27$, two-tailed) comparing 20 kDa dextran through Nsp1-modified PLY-DNA pores (median = 1.64 $nm \cdot min^{-1}$, $n = 16$) and 40 kDa dextran through Nsp1-modified PLY-DNA pores (median = 0.50 $nm \cdot min^{-1}$, $n = 16$)

DIFFUSION MODEL

FRAP traces from 7 individual GUVs were fitted with an established diffusion model[9] using MATLAB:

$$\frac{c_{out} - c_{in}(t)}{c_{out}} = \left(1 - \frac{c_{in,start}}{c_{out}}\right) e^{-\left(\frac{D_{eff} \times A \times N}{V \times L}\right)t}$$

where c_{out} and c_{in} refer to the concentrations of dextran molecules outside and inside each GUV, respectively.

The concentration difference $\left(\frac{c_{out} - c_{in}(t)}{c_{out}}\right)$ across time points (t) post-photobleaching was measured as shown in **Figure S10**.

A is the inner area of PLY-DNA pores, calculated from our cryo-EM measurements of 22 nm pore diameter to be 380.1 nm^2.

V is the volume of a GUV, calculated from the measured GUV diameter.

The effective diffusion constant D_{eff} for the 20 kDa dextran was calculated based on a previously described formula[10]:

$$\frac{D_{eff}}{D_{bulk}} = 1 + \frac{9}{8}\left(\frac{R_g}{R_p}\right)\ln\left(\frac{R_g}{R_p}\right) - 1.56034\left(\frac{R_g}{R_p}\right) + 0.528155\left(\frac{R_g}{R_p}\right)^2 + 1.91521\left(\frac{R_g}{R_p}\right)^3 - 2.81903\left(\frac{R_g}{R_p}\right)^4 + 0.270788\left(\frac{R_g}{R_p}\right)^5 + 1.10115\left(\frac{R_g}{R_p}\right)^6 - 0.435933\left(\frac{R_g}{R_p}\right)^7$$

in which the diffusion constant of the dextran in solution (D_{bulk}) was previously reported[11] to be 44 μm^2/s. The radius of gyration (R_g) for 20 kDa dextran is 4.2 nm while the radius of the PLY-DNA pore (R_p) is 11 nm. This yields an effective diffusion constant D_{eff} of 5.26 μm^2/s for the 20 kDa dextran.

L from the diffusion model refers to the PLY-DNA pore's channel length. As the height of the DNA origami ring is 14 nm, and the height of the PLY ring is 11 nm (ref [4]), L is estimated to be up to 25 nm when including both the DNA origami and its corralled PLY pore. The lower bound for L is 11 nm if the channel length contribution from the DNA origami portion is completely disregarded.

Finally, with the $\left(\frac{D_{eff} \times A \times N}{V \times L}\right)$ obtained from mathematical fitting, N (the number of pores on each GUV) could then be determined. The pore density was estimated to be between 0.25±0.15/μm^2 (L = 11 nm) and 0.56±0.34/μm^2 (L = 25 nm).

REFERENCES

(1) Douglas, S. M.; Marblestone, A. H.; Teerapittayanon, S.; Vazquez, A.; Church, G. M.; Shih, W. M. Rapid prototyping of 3D DNA-origami shapes with caDNAno. *Nucleic Acids Res* **2009**, *37* (15), 5001-5006. DOI: 10.1093/nar/gkp436

(2) Douglas, S. M.; Dietz, H.; Liedl, T.; Hogberg, B.; Graf, F.; Shih, W. M. Self-assembly of DNA into nanoscale three-dimensional shapes (vol 459, pg 414, 2009). *Nature* **2009**, *459* (7250), 1154-1154. DOI: 10.1038/nature08165

(3) Lin, C.; Perrault, S. D.; Kwak, M.; Graf, F.; Shih, W. M. Purification of DNA-origami nanostructures by rate-zonal centrifugation. *Nucleic Acids Res* **2013**, *41* (2), e40. DOI: 10.1093/nar/gks1070

(4) van Pee, K.; Neuhaus, A.; D'Imprima, E.; Mills, D. J.; Kuhlbrandt, W.; Yildiz, O. CryoEM structures of membrane pore and prepore complex reveal cytolytic mechanism of Pneumolysin. *Elife* **2017**, *6*. DOI: 10.7554/eLife.23644

(5) Shen, Q.; Tian, T.; Xiong, Q.; Ellis Fisher, P. D.; Xiong, Y.; Melia, T. J.; Lusk, C. P.; Lin, C. DNA-Origami NanoTrap for Studying the Selective Barriers Formed by Phenylalanine-Glycine-Rich Nucleoporins. *J Am Chem Soc* **2021**, *143* (31), 12294-12303. DOI: 10.1021/jacs.1c05550

(6) Darji, A.; Chakraborty, T.; Niebuhr, K.; Tsonis, N.; Wehland, J.; Weiss, S. Hyperexpression of listeriolysin in the nonpathogenic species Listeria innocua and high yield purification. *J Biotechnol* **1995**, *43* (3), 205-212. DOI: 10.1016/0168-1656(95)00138-7

(7) Angelova, M. I.; Soleau, S.; Meleard, P.; Faucon, J. F.; Bothorel, P. Preparation of Giant Vesicles by External Ac Electric-Fields - Kinetics and Applications. *Prog Coll Pol Sci S* **1992**, *89*, 127-131.

(8) Schneider, C. A.; Rasband, W. S.; Eliceiri, K. W. NIH Image to ImageJ: 25 years of image analysis. *Nat Methods* **2012**, *9* (7), 671-675. DOI: 10.1038/nmeth.2089

(9) Fragasso, A.; De Franceschi, N.; Stommer, P.; van der Sluis, E. O.; Dietz, H.; Dekker, C. Reconstitution of Ultrawide DNA Origami Pores in Liposomes for Transmembrane Transport of Macromolecules. *Acs Nano* **2021**, *15* (8), 12768-12779. DOI: 10.1021/acsnano.1c01669

(10) Dechadilok, P.; Deen, W. M. Hindrance factors for diffusion and convection in pores. *Ind Eng Chem Res* **2006**, *45* (21), 6953-6959. DOI: 10.1021/ie051387n

(11) Silva, J. V. C.; Peixoto, P. D. S.; Lortal, S.; Floury, J. Transport phenomena in a model cheese: The influence of the charge and shape of solutes on diffusion. *J Dairy Sci* **2013**, *96* (10), 6186-6198. DOI: 10.3168/jds.2013-6552